An ecohydrologic model for a shallow groundwater urban environment

Sam Arden, Xin (Cissy) Ma and Mark Brown

ABSTRACT

The urban environment is a patchwork of natural and artificial surfaces that results in complex interactions with and impacts to natural hydrologic cycles. Evapotranspiration is a major hydrologic flow that is often altered through urbanization, although the mechanisms of change are sometimes difficult to tease out due to difficulty in effectively simulating soil–plant–atmosphere interactions. This paper introduces a simplified yet realistic model that is a combination of existing surface runoff and ecohydrology models designed to increase the quantitative understanding of complex urban hydrologic processes. Results demonstrate that the model is capable of simulating the long-term variability of major hydrologic fluxes as a function of impervious surface, temperature, water table elevation, canopy interception, soil characteristics, precipitation and complex mechanisms of plant water uptake. These understandings have potential implications for holistic urban water system management.

Key words | ecohydrology, evapotranspiration, shallow groundwater, urban heat island, urban, vegetation covers

Sam Arden (corresponding author)
Mark Brown
UF Center for Environmental Policy,
102 Phelps Laboratory,
University of Florida,
P.O. Box 116350,
Gainesville,
FL 32611-6350,
USA
E-mail: *sarden@ufl.edu*

Xin (Cissy) Ma
US EPA ORD,
National Risk Management Research Laboratory,
Sustainable Technology Division,
26 West Martin Luther King Drive,
Mail Stop 483,
Cincinnati,
Ohio 45268,
USA

INTRODUCTION

The urban environment is a heterogeneous patchwork of natural and artificial surfaces that results in complex interactions with and impacts to the hydrologic cycle (Grimmond & Oke 1999; Arnfield 2003). For example, urbanization replaces vegetated surfaces with impervious built surfaces, altering natural processes such as evaporative cooling, rainwater interception, storage and infiltration functions (Gill *et al.* 2007). When urbanization occurs in areas where groundwater plays a key role in hydrologic and ecosystem function, understanding the dynamic interactions between precipitation, soil water content, vegetation and the built environment is a critical aspect of surface and groundwater resource management. Currently, there are few process-based models that can effectively simulate the soil–plant–atmosphere system (Soylu *et al.* 2014), particularly in an urban setting.

Due to these complex interactions, one component of the hydrologic budget that is particularly difficult to characterize is evapotranspiration (ET), or the combination of evaporation and vegetation-mediated transpiration. Despite the presence of non-evaporative surfaces, ET remains a significant component of the urban water budget (Grimmond & Oke 1999; Boggs & Sun 2011). Changes in ET due to urbanization result in numerous direct and indirect environmental impacts, including downstream water quality impacts (Carpenter *et al.* 1998) and increased ambient temperatures resulting in the urban heat island effect (UHI) (Taha 1997; Arnfield 2003; Ban-Weiss *et al.* 2011).

Not properly accounting for soil–plant–atmosphere interactions can lead to incorrect estimates of land surface hydrologic fluxes (Yeh & Eltahir 2005; Maxwell & Kollet 2008), including ET. In shallow groundwater environments, soil moisture can be an important source of water for plants (Rodriguez-Iturbe *et al.* 2007; Lowry & Loheide 2010), and can maintain transpiration during dry times (Soylu *et al.* 2014). This subsidy can come from both saturated and unsaturated zones of the soil column, and is a function of soil moisture, soil properties and plant physiology (Orellana *et al.* 2012). However, detailed understanding of the partitioning of transpiration between saturated and unsaturated zones is limited and requires development of integrated models able to link hydrology, ecology and geomorphology (Orellana *et al.* 2012).

doi: 10.2166/wst.2014.299

Existing models designed to simulate soil–plant–atmosphere interactions can be grouped into categories of variably saturated, saturated, fully distributed and lumped models. Orellana *et al.* (2012) provide a review of such models, highlighting strengths and weaknesses of each. Although all approaches have their merits, lumped models are identified as a less detailed and more theoretical approach designed to understand the key processes linking soil, vegetation and climate variability using a reduced number of parameters. It is recognized that understanding these processes is a fundamental requirement of hydrology and ecology (Rodriguez-Iturbe *et al.* 2007). Without such holistic and fundamental understanding, it will be difficult to develop effective and sustainable urban water management strategies (Odum & Barrett 2005; US EPA 2003, 2008).

Recent works in the ecohydrology field have applied a framework first developed by Rodriguez-Iturbe *et al.* (1999) to study the interactions between precipitation, soil water content and vegetation in both arid ecosystems (Rodriguez-Iturbe & Porporato 2004) and humid groundwater-dependent ecosystems (Laio *et al.* 2009). In comparison to variably saturated, saturated or fully distributed and coupled hydrologic models, the lumped model framework developed by Rodriguez-Iturbe *et al.* (1999) and further refined by Laio *et al.* (2009) allows for clear interpretation of the interactions between groundwater, soil moisture, vegetation and precipitation variability using a simple yet realistic and mathematically tractable approach (Orellana *et al.* 2012). Although successfully applied in the Everglades, Florida, to reproduce water table fluctuations (Pumo *et al.* 2010; Tamea *et al.* 2010), the framework has not been applied to the urban system.

This paper is intended to introduce and show the basic capabilities of a physically-based lumped model designed to simulate natural soil–plant–atmosphere interactions in an urban setting influenced by shallow groundwater tables. By using a spatially simple yet ecohydrologically realistic model, a better understanding of the complex interactions between natural and built systems can be provided, which can lead to more effective urban water management.

METHODS

Model description

A one-dimensional stochastic model was created by integrating existing runoff (Soil Conservation Service (SC) curve number (CN) method; USDA 1986), soil moisture (Laio *et al.* 2001) and water table (Laio *et al.* 2009) models to investigate the effects of urbanization under conditions of an idealized landscape. Following Laio *et al.* (2009) a simplified plot of unit area (horizontal area of interest on the order of 1–100 m^2) was assumed, which is also applicable to the household or plot scale. Topographical variation was assumed to be negligible, soil composition was assumed to be vertically and horizontally homogeneous, and vegetation cover on vegetated areas was assumed to be spatially uniform. Three types of soil (sand, loamy sand and loam) as well as three types of vegetation cover (grass, shrub and tree) were used as inputs into the model to show the effects of urbanization given a range of environmental conditions. The model was designed to run at a daily time-step to capture relevant hydrologic fluxes with simulation periods of 100 years to allow for more precise characterization of long-term trends.

Climate

Daily rainfall and potential evapotranspiration (PET) were defined for the model and assumed to be spatially uniform. Following Rodriguez-Iturbe *et al.* (1999), daily rainfall was modeled as a stochastic Poisson process, $P(\lambda, \alpha)$, where the interval between individual rainfall events follows a Poisson distribution of frequency λ and the depth of individual rainfall events follows an exponential probability distribution of mean depth α. This paper uses data from North Central Florida (Florida Automated Weather Network; http://fawn.ifas.ufl.edu, Station: Alachua) to constrain the results within locally realistic climate conditions. Based on data from 2003–2012, average annual rainfall was 1.27 m, α was determined to be approximately 0.011 m and a value of 0.60 for λ was back-calculated. To account for seasonal variability, monthly rainfall averages were determined and α was adjusted accordingly, resulting in values of α ranging from 0.041 m in November to 0.22 m in June. PET was determined using the Priestley Taylor method (Douglas *et al.* 2009), which defines daily PET as a function of daily solar radiation, mean temperature, minimum temperature and a number of environmental constants. Daily temperature and radiation data were obtained from the above-mentioned weather station, and resulted in an average annual PET of 1.72 m.

Surface runoff, interception and infiltration

In an urban environment, the amount of infiltration to the soil column depends first on the initial abstraction and runoff characteristics of the landscape, which are both a function of vegetation type and land use cover. Surface runoff (R) was calculated using the SCS CN method, which provides a simplified set of equations for characterizing runoff from small urbanizing watersheds (USDA 1986). Curve numbers were selected from the TR-55 manual assuming fair conditions and C-group soils, yielding a CN of 73, 70, and 79 for tree, shrub and grass covers, respectively (USDA 1986). Antecedent moisture conditions were not applied, as soil moisture was explicitly modeled and allowed for direct calculation of increased infiltration capacity during dry conditions and increased runoff generation during saturated conditions.

Once surface runoff was partitioned from precipitation, the portion remaining on the landscape (the initial abstraction term from the CN equation) was further subdivided into interception and infiltration. Canopy interception (I_c), or the portion of intercepted precipitation that evaporates without reaching the soil (Klaassen *et al.* 1998), can account for a significant fraction of the precipitation on forests. An I_c value of 1.6 mm was applied to the tree vegetation cover, which is representative of mixed hardwood forest stands of the southeastern USA (Bryant *et al.* 2005). In the model, this term serves as a temporary storage that must be filled before infiltration occurs, and evaporated before it can be filled again (provided there is sufficient evaporative demand, or PET). To account for the difference in leaf coverage, I_c for shrub cover was set to half of tree cover (0.8 mm) and grass I_c was assumed to be negligible (0 mm). Depressional storage was not included in this application, although can be added as an additional interception term and used as a sort of calibration parameter to help account for topographical variation and variation in infiltration rates due to vegetation cover.

For simulations testing the effects of impervious surface cover, a unit area was assumed for each simulation and a portion of that area was assigned a CN of 100. Any precipitation falling on this impervious surface was then directed to the vegetated portion of the unit area (assumption of 0% directly connected impervious area, or DCIA) and incorporated into the SCS runoff equation as follows:

$$R_{imp} = P \cdot \%imp \tag{1}$$

$$P_{veg} = P + R_{imp} \tag{2}$$

where R_{imp} is the runoff generated from the impervious surface, P is precipitation and P_{veg} is the adjusted precipitation amount falling on the vegetated surface that is used as input to the SCS runoff equation.

Soil moisture in the low moisture zone

Subsurface water table and soil moisture were modeled following a framework proposed by Laio *et al.* (2009) and Laio *et al.* (2001), respectively, which divides the soil column into three zones according to local water content (Figure 1).

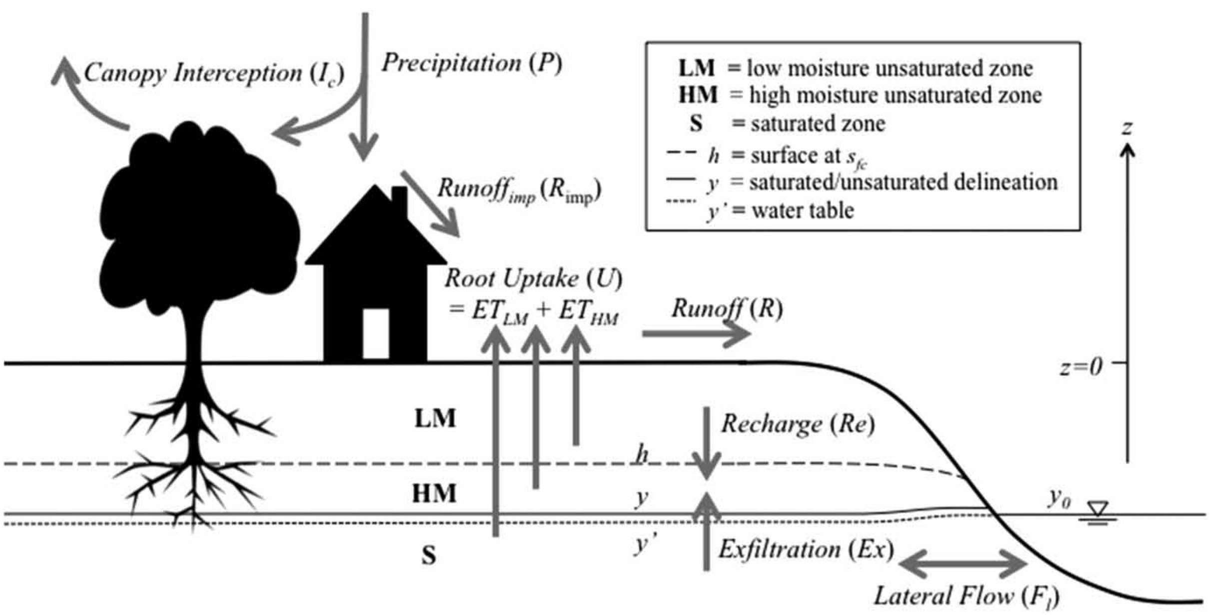

Figure 1 | Schematic of soil column and model framework (adapted from Laio *et al.* 2009).

Starting from the bottom is the saturated zone (S), where all soil pore space is filled with water (i.e. soil moisture, $s = 1$). The upper boundary of the saturated zone (denoted as y) is defined as the water table depth. This is calculated as the sum of the saturated soil surface at zero pressure (denoted as y' in Figure 1) plus the negative soil matric potential (Ψ_s). Above the saturated zone is the high moisture unsaturated zone (HM), where soil moisture is greater than field capacity (s_{fc}) but less than saturation (i.e. $s_{fc} \leq s < 1$). Lastly is the low moisture unsaturated zone (LM) where soil moisture is less than field capacity (i.e. $s < s_{fc}$). The delineation between the HM and LM zones is denoted as h. Following Laio *et al.* (2009), the LM zone only develops when $y < y_c$, where y_c is a critical depth and is a function of soil properties and vegetation rooting depth. A further key distinction between the two zones is that the HM zone is characterized by large values of hydraulic conductivity (assumption of 'instantaneous' water transmission on the daily scale) while in the LM zone the hydraulic conductivity is assumed to be negligible, yet large enough to allow for uniform redistribution of soil moisture at the daily time scale.

The LM zone was modeled separately from the HM and saturated zones, as recharge to the lower zones is a function of LM zone soil moisture; when $s > s_{fc}$ in the LM zone, excess precipitation recharges to the HM zone. In effect, the LM zone acts as a filtering reservoir above the HM zone that must be filled ($s > s_{fc}$) before precipitation can recharge to the zones below. Accordingly, a simple water balance model was developed similar to Laio *et al.* (2001) to calculate daily soil moisture in the LM zone

$$s_{t+1} = s_t + \frac{ds}{dt} \tag{3}$$

$$Inf = P_{veg} - I_c - R \tag{4}$$

$$-nh\frac{ds}{dt} = \left(P_{veg} - I_c - R\right) - ET_{LM} - Re \tag{5}$$

where Inf is the amount of adjusted precipitation that is able to infiltrate into the low moisture zone of the vegetated area, n is soil porosity, R is runoff, ET_{LM} is the ET from the LM zone and Re is recharge, or the amount of incoming water that cannot be stored in the LM zone and recharges to the HM zone. Following the assumption that when soil moisture is greater than field capacity ($s > s_{fc}$) conductivities are large enough to allow for instantaneous water distribution at the daily time scale, LM storage is calculated as $-nh(s_{fc} - s)$ and any excess incoming flow is immediately routed to the HM zone.

ET from the LM zone is calculated as a function of soil moisture, remaining evaporative demand (i.e. the portion of PET not consumed by initial abstraction, in this case I_c), and theoretical plant uptake dynamics. Assuming ET_{LM} decreases linearly from ($PET - I_c$) at $s = s_{fc}$ to 0 when soil moisture reaches the wilting point (s_w) (Laio *et al.* 2001), ET_{LM} was modeled as

$$ET_{LM} = (PET - I_c)*\frac{(s - s_w)}{(s_{fc} - s_w)} \tag{6}$$

Shallow groundwater table

The shallow groundwater table was simulated following Laio *et al.* (2009), where a water balance is generated around the water table surface (y) and the boundary between the HM and LM zones (h) is calculated as a function of y and y_c. The water balance was calculated as

$$y_{t+1} = y_t + \frac{dy}{dt} \tag{7}$$

$$\beta\frac{dy}{dt} = Re - F_l - ET_{HM} \tag{8}$$

where β is specific yield, F_l is lateral groundwater flow into (negative) or out of (positive) the system, and ET_{HM} is the ET flux from the HM and saturated zones. Specific yield (β) was modeled as a function of soil properties and water depth following Laio *et al.* (2009).

Lateral flow into or out of the system was calculated assuming there was a constant water surface at elevation y_0 some distance, dL, away from the system (see Figure 1). Because the model is one-dimensional, flow was calculated using a modified Darcy's equation

$$F_l = k_s\frac{(y_o - y')}{dL} \tag{9}$$

where k_s is the saturated hydraulic conductivity (see Table 1). A value of 1,000 m was assumed for dL for all simulations, with the intention of simulating an urban environment with an artificially imposed surface water feature at some reasonable distance from the plot scale (stormwater pond, drainage ditch, etc.).

Table 1 | Model soil input parameters[a]

Parameter	Sand	Loamy sand	Loam
k_s (m/day)	15.2	13.5	0.6
Ψ_s (−m)	0.12	0.09	0.48
s_{fc} (m/m)	0.44	0.44	0.70
s_w (m/m)	0.17	0.18	0.34
n (m/m)	0.40	0.41	0.45

[a]Clapp & Hornberger (1978). k_s is saturated hydraulic conductivity, Ψ_s is saturated soil matric potential, s_{fc} is soil moisture content at field capacity, s_w is soil moisture content at wilting point and n is soil porosity.

Based on the remaining evaporative demand ($PET - I_c - ET_{LM}$), ET from the HM and saturated zones was calculated as the sum of root uptake (U) and exfiltration (Ex) (see Laio *et al.* (2009) for additional discussion)

$$ET_{HM} = (PET - I_c - ET_{LM})e^{h/b} \quad (10)$$

where b is the average rooting depth. The derivations of the governing equations assume that root biomass is represented by an exponential distribution of form $r(z) = (1/b)e^{z/b}$, which has been reported and used by other authors (e.g. Schenk & Jackson 2002; Laio 2006). The total ET flux can then be calculated as $I_c + ET_{LM} + ET_{HM}$. For the model simulations presented next, it was assumed that the tree vegetation cover had a mean rooting depth of 40 cm, which is representative of flatwoods ecosystems typically found in north Florida (Van Rees & Comerford 1986). In order to compare the effects of typical urban vegetation cover on ET fluxes, it was assumed that the mean rooting depth of the grass cover was 10 cm. Although turfgrass root distributions have been rarely quantified in the literature, it has been documented that grasses in non-arid environments typically have shallower roots than trees (Zhang *et al.* 2001; Jackson *et al.* 1996). Furthermore, it has been suggested that land conversions from tall canopies (e.g. natural forest) to short canopies decreases maximum root depth (Moore & Heilman 2011). For comparative purposes, it was assumed that the mean rooting depth of the shrub cover was midway between tree and grass, or 25 cm.

The model was run in Microsoft Excel for a variety of inputs to show the relative effect of factors such as soil, vegetation cover, water table elevation, temperature and impervious surface cover on ET fluxes. To test the effects of groundwater, water table elevations (y_0) were varied from −0.5 to −3.0 m. To test the effects of the UHI, temperature inputs for daily PET calculations were raised at 2 °C increments to a maximum of 10 °C; the lower bound being consistent with numerous observations, the upper bound being representative of a maximum increase discussed in Shepherd (2005). To test the effects of impervious surface cover, the percent of the plot covered with impervious surface was varied from 0 to 50%, under conditions of 0% DCIA and 100% DCIA to show the mitigating effects that could be provided by directing impervious surface runoff to vegetated surfaces.

RESULTS AND DISCUSSION

Vegetation and soil type

As a first step the model was run assuming a shallow groundwater table of −2 m ($y_0 = -2$) and 0% impervious surface cover. The results are given in Figure 2, which shows the effect of soil type and vegetation cover on total average annual ET flux (calculated as $I_c + ET_{LM} + ET_{HM}$).

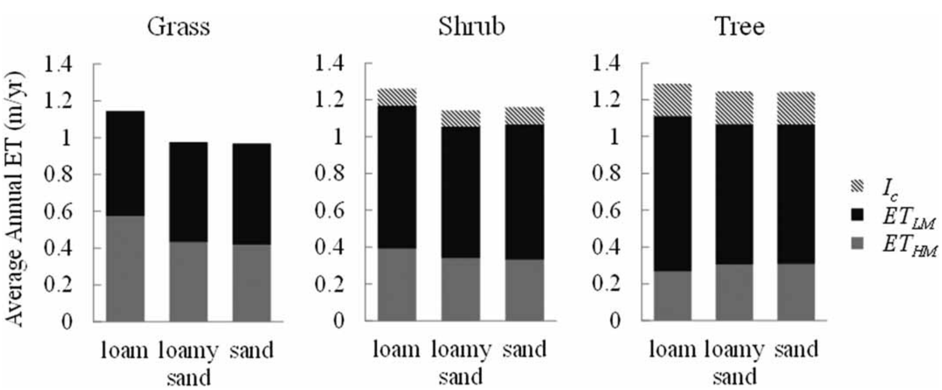

Figure 2 | Average annual ET by vegetation cover and soil type. ET was composed of canopy interception (I_c), ET from the low moisture zone (ET_{LM}) and ET from the high moisture zone (ET_{HM}). Water table elevation (y_0) = −2.0 m.

As can be seen from Figure 2, vegetation with a greater canopy coverage and deeper rooting depth (e.g. tree) maintains a greater ET flux throughout the year, which is consistent with results of numerous paired catchment studies (Brown *et al.* 2005). In addition to vegetation cover, the model demonstrates the importance of soil types on ET (Chen *et al.* 2014), as changes in annual ET are more pronounced for loamy sand and sand soils when vegetation is varied.

Figure 2 also shows the partitioning of total ET to the three components – canopy interception (I_c), ET from the low moisture/unsaturated zone (ET_{LM}) and ET from the high moisture/saturated zone (ET_{HM}). In general, the moisture contribution to ET from the unsaturated zone (ET_{LM}) is the greatest across soil and vegetation type, stressing the importance of properly characterizing unsaturated soil moisture dynamics, as contributions to plant transpiration from this zone can be significant (Soylu *et al.* 2011). Although variably saturated models such as HYDRUS (Simunek *et al.* 2009) have been used to simulate soil moisture–plant interactions, their root uptake term generally do not take into account the realistic distribution of root biomass (i.e. exponential decay). This drawback was specifically identified by Shah *et al.* (2007) who used HYDRUS to show that the decline in groundwater-dependent plant transpiration with declining water tables was better represented by an exponential decay function, not a linear decay function as is commonly used in similar models (Orellana *et al.* 2012).

Water table elevation

Figure 3(a) shows the effect of various water table depths on annual ET/PET for loamy sand soils. The results show that when groundwater tables are shallow, water limitation of both deep and shallow rooting vegetation may be reduced, as adjacent water features can supplement a portion of the water required to maintain high ET rates during dry periods. As water tables decrease, simulation results suggest that ET rates from shallow-rooted vegetation decrease nonlinearly more than that from deeper rooted vegetation, as the shallow roots are less able to access deeper sources of water and capillary fluxes are not able to satisfy plant demand. This implies that as water tables decrease, trees may be more effective than grass at maintaining ET fluxes during dry periods (counteracting UHI effects) and may reduce annual runoff rates as more incoming precipitation is ultimately routed to ET (Booth *et al.* 2002; Brown *et al.* 2005). The idea that vegetation type exerts greater control on annual ET under water-limited conditions is also consistent

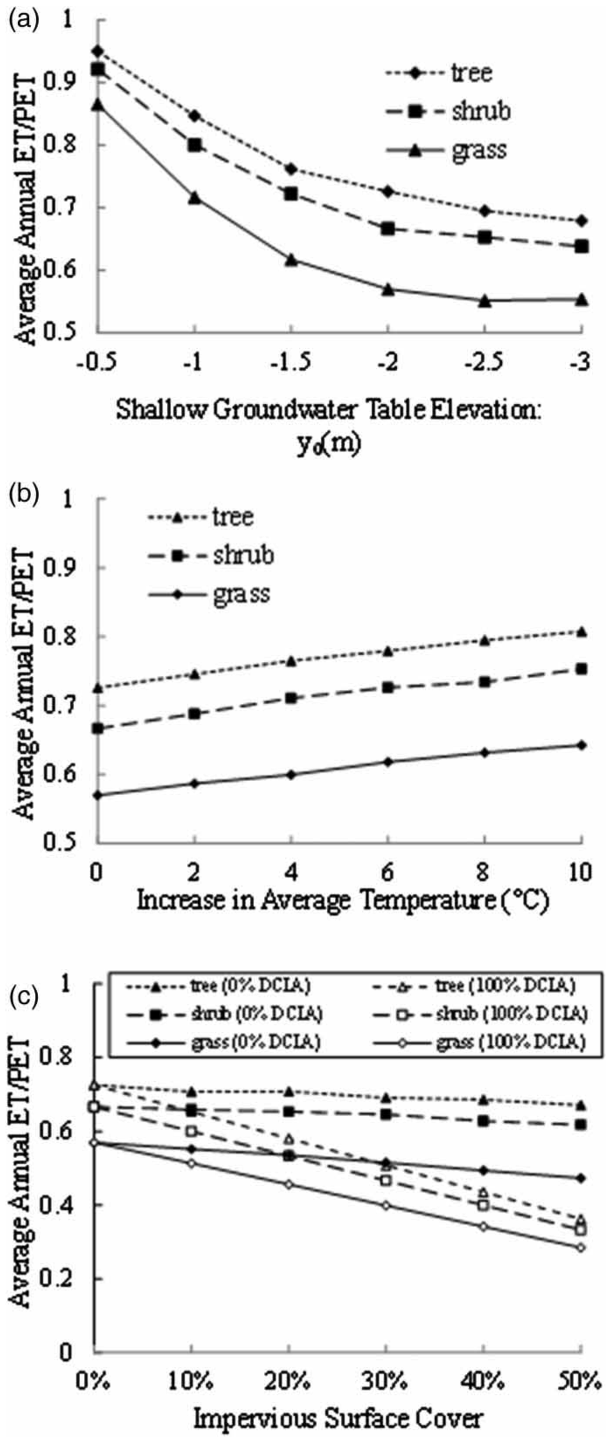

Figure 3 | (a) Average annual ET/PET for a range of shallow groundwater table (y_0) conditions. Simulation results for loamy sand soil type. (b) Average annual ET/PET for a range of ambient temperature conditions. PET was modified through increases in both average and minimum temperature inputs for the ranges given. Simulation results for loamy sand soil type. Water table elevation (y_0) = −2.0 m. (c) Average annual ET/PET for a range of impervious surface coverage conditions. Results shown for 0% and 100% DCIA. Simulation results for loamy sand soil type. Water table elevation (y_0) = −2.0 m.

with previous research (Gill *et al.* 2007; House-Peters & Chang 2011; Moore & Heilman 2011).

Temperature (UHI)

Results shown in Figure 3(b) suggest that increases in ambient temperature will increase ET fluxes from vegetated surfaces, so long as water is not limiting. Results suggest that for every 1 °C increase, ET/PET will increase by approximately 1%, and effects appear to be similar for all vegetation types. Although not a large increase, when considered in the context of the complex urban environment this result may point to several more critical consequences. First, shallow-rooted vegetation such as grass may deplete shallow soil moisture stores more rapidly, requiring additional water inputs (irrigation), leading to increased water consumption. Second, if increases in PET occur without concurrent increases in water supply, the amount of incoming radiation converted to sensible heat may increase (through a decrease in latent heat), representing a positive feedback loop that may further exacerbate UHI effects.

Impervious surface cover

A final but significant component of urban areas assessed in this paper is impervious cover. The results presented in Figure 3(c) show that for cases of 0% DCIA, as impervious surface increases, the plot-scale (i.e. ET flux normalized to impervious + vegetated area) ET does not decrease at a 1:1 rate with the concurrent decrease in vegetated area. For example, at 50% impervious surface under 0% DCIA, the plot-scale ET/PET flux decreases 17, 7 and 8% for grass, shrub and tree covers, respectively. Compared to 100% DCIA (i.e. roof runoff flows directly off-site), at 50% impervious surface cover the plot-scale ET/PET flux would decrease 50%. This is because under 0% DCIA conditions, water generated on-site from impervious surfaces is used as a supplemental hydrologic input to the vegetated areas, which increases the annual ET rate from the vegetated surface through increased water table elevations and available soil moisture. Although this is somewhat intuitive, it highlights the ability of the model to capture complex feedbacks between urban and natural systems.

CONCLUSION

This paper has introduced a model designed to increase the quantitative understanding of the complex dynamics present in an urban environment using a novel combination of simple yet realistic surface runoff and ecohydrologic models. Although this paper focuses on the nuances of soil–plant–atmosphere interactions vis-à-vis ET, the model is capable of simulating the long-term variability of major hydrologic fluxes as a function of impervious surface, temperature, water table elevation, canopy interception, soil characteristics, precipitation and complex mechanisms of plant water uptake. Such an integrated yet relatively simple model is essential to improving our fundamental understanding of urban hydrologic processes and to further develop more effective urban water management strategies using a holistic approach. Although the general results presented are by no means surprising, this paper was intended to demonstrate the types of problems this model can potentially address. Ultimately, the understanding of these interactions in the model can complement other commonly used urban land surface models such as the EPA Storm Water Management Model. Future studies are needed to validate the model using empirical data as well as to provide insight into more sustainable urban water systems.

Disclaimer

This publication was developed under EPA's National Network for Environmental Management Studies Fellowship No. 2013-301. The views expressed in this document are solely those of the authors and EPA does not endorse any products or commercial services mentioned in this publication.

REFERENCES

Arnfield, A. J. 2003 Two decades of urban climate research: a review of turbulence, exchanges of energy and water, and the urban heat island. *International Journal of Climatology* **23** (1), 1–26.

Ban-Weiss, G. A., Bala, G., Cao, L., Pongratz, J. & Caldeira, K. 2011 Climate forcing and response to idealized changes in surface latent and sensible heat. *Environmental Research Letters* **6** (3), 8.

Boggs, J. L. & Sun, G. 2011 Urbanization alters watershed hydrology in the Piedmont of North Carolina. *Ecohydrology* **4** (2), 256–264.

Booth, D. B., Hartley, D. & Jackson, R. 2002 Forest cover, impervious-surface area, and the mitigation of stormwater impacts. *JAWRA Journal of the American Water Resources Association* **38** (3), 835–845.

Brown, A. E., Zhang, L., McMahon, T. A., Western, A. W. & Vertessy, R. A. 2005 A review of paired catchment studies for determining changes in water yield resulting from alterations in vegetation. *Journal of Hydrology* **310** (1–4), 28–61.

Bryant, M. L., Bhat, S. & Jacobs, J. M. 2005 Measurements and modeling of throughfall variability for five forest communities in the southeastern US. *Journal of Hydrology* **312** (1–4), 95–108.

Carpenter, S. R., Caraco, N. F., Correll, D. L., Howarth, R. W., Sharpley, A. N. & Smith, V. H. 1998 Nonpoint pollution of surface waters with phosphorus and nitrogen. *Ecological Applications* **8** (3), 559–568.

Chen, M., Willgoose, G. R. & Saco, P. M. 2014 Spatial prediction of temporal soil moisture dynamics using HYDRUS-1D. *Hydrological Processes* **28** (2), 171–185.

Clapp, R. B. & Hornberger, G. M. 1978 Empirical equations for some soil hydraulic properties. *Water Resources Research* **14** (4), 601–604.

Douglas, E. M., Jacobs, J. M., Sumner, D. M. & Ray, R. L. 2009 A comparison of models for estimating potential evapotranspiration for Florida land cover types. *Journal of Hydrology* **373** (3–4), 366–376.

Gill, S. E., Handley, J. F., Ennos, A. R. & Pauleit, S. 2007 Adapting cities for climate change: the role of the green infrastructure. *Built Environment* **33** (1), 115–133.

Grimmond, C. S. B. & Oke, T. R. 1999 Evapotranspiration rates in urban areas. In: *Impacts of Urban Growth on Surface Water and Groundwater Quality: Proceedings of IUGG 99 Symposium HS5, Birmingham*.

House-Peters, L. A. & Chang, H. 2011 Modeling the impact of land use and climate change on neighborhood-scale evaporation and nighttime cooling: a surface energy balance approach. *Landscape and Urban Planning* **103** (2), 139–155.

Jackson, R. B., Canadell, J., Ehleringer, J. R., Mooney, H. A., Sala, O. E. & Schulze, E. D. 1996 A global analysis of root distributions for terrestrial biomes. *Oecologia* **108** (3), 389–411.

Klaassen, W., Bosveld, F. & de Water, E. 1998 Water storage and evaporation as constituents of rainfall interception. *Journal of Hydrology* **212** (1–4), 36–50.

Laio, F. 2006 A vertically extended stochastic model of soil moisture in the root zone. *Water Resources Research* **42** (2), art. W02406, doi:10.1029/2005WR004502.

Laio, F., Porporato, A., Ridolfi, L. & Rodriguez-Iturbe, I. 2001 Plants in water-controlled ecosystems: active role in hydrologic processes and response to water stress – II. Probabilistic soil moisture dynamics. *Advances in Water Resources* **24** (7), 707–723.

Laio, F., Tamea, S., Ridolfi, L., D'Odorico, P. & Rodriguez-Iturbe, I. 2009 Ecohydrology of groundwater-dependent ecosystems: 1. Stochastic water table dynamics. *Water Resources Research* **45**, art. W05419, doi:10.1029/2008WR007292.

Lowry, C. S. & Loheide, S. P. 2010 Groundwater-dependent vegetation: quantifying the groundwater subsidy. *Water Resources Research* **46**, art. W06202, doi:10.1029/2009wr008874.

Maxwell, R. M. & Kollet, S. J. 2008 Interdependence of groundwater dynamics and land-energy feedbacks under climate change. *Nature Geoscience* **1** (10), 665–669.

Moore, G. W. & Heilman, J. L. 2011 Proposed principles governing how vegetation changes affect transpiration. *Ecohydrology* **4** (3), 351–358.

Odum, E. P. & Barrett, G. W. 2005 *Fundamentals of Ecology* 5th edn. Peter Marshall, Brooks/Coles, Belmont, Canada.

Orellana, F., Verma, P., Loheide, S. P. & Daly, E. 2012 Monitoring and modeling water-vegetation interactions in groundwater-dependent ecosystems. *Reviews of Geophysics* **50**, art. Rg3003, doi:10.1029/2011rg000383.

Pumo, D., Tamea, S., Noto, L. V., Miralles-Wilhem, F. & Rodriguez-Iturbe, I. 2010 Modeling belowground water table fluctuations in the Everglades. *Water Resources Research* **46**, art. W11557, doi:10.1029/2009wr008911.

Rodriguez-Iturbe, I. & Porporato, A. 2004 *Ecohydrology of Water-Controlled Ecosystems: Soil Moisture and Plant Dynamics*. Cambridge University Press, Cambridge, UK.

Rodriguez-Iturbe, I., Porporato, A., Ridolfi, L., Isham, V. & Cox, D. R. 1999 Probabilistic modelling of water balance at a point: the role of climate, soil and vegetation. *Proceedings of the Royal Society A – Mathematical Physical and Engineering Sciences* **455** (1990), 3789–3805.

Rodriguez-Iturbe, I., D'Odorico, P., Laio, F., Ridolfi, L. & Tamea, S. 2007 Challenges in humid land ecohydrology: interactions of water table and unsaturated zone with climate, soil, and vegetation. *Water Resources Research* **43** (9), art. W09301, doi:10.1029/2007wr006073.

Schenk, H. J. & Jackson, R. B. 2002 The global biogeography of roots. *Ecological Monographs* **72** (3), 311–328.

Shah, N., Nachabe, M. & Ross, M. 2007 Extinction depth and evapotranspiration from ground water under selected land covers. *Ground Water* **45** (3), 329–338.

Shephard, J. M. 2005 A review of current investigations of urban-induced rainfall and recommendations for the future. *Earth Interactions* **9**, paper no. 12.

Simunek, J., van Genuchten, M. T. & Sejna, M. 2009 *The HYDRUS-1D Software Package for Simulating the One Dimensional Movement of Water, Heat and Multiple Solutes in Variably Saturated Media*. Technical Report, Department of Environ. Sci., University of California, Riverside, CA, USA.

Soylu, M. E., Istanbulluoglu, E., Lenters, J. D. & Wang, T. 2011 Quantifying the impact of groundwater depth on evapotranspiration in a semi-arid grassland region. *Hydrology and Earth System Sciences* **15** (3), 787–806.

Soylu, M. E., Kucharik, C. J. & Loheide, S. P. 2014 Influence of groundwater on plant water use and productivity: development of an integrated ecosystem – variably saturated soil water flow model. *Agricultural and Forest Meteorology* **189**, 198–210.

Taha, H. 1997 Urban climates and heat islands: Albedo, evapotranspiration, and anthropogenic heat. *Energy and Buildings* **25** (2), 99–103.

Tamea, S., Muneepeerakul, R., Laio, F., Ridolfi, L. & Rodriguez-Iturbe, I. 2010 Stochastic description of water table fluctuations in wetlands. *Geophysical Research Letters* **37**, art. W05420, doi:10.1029/2008wr007293.

USDA (US Department of Agriculture) 1986 *Urban Hydrology for Small Watersheds*. Technical Release 55, Conservation Engineering Division, USDA National Resource Conservation Service, Washington, DC, USA.

US EPA (Environmental Protection Agency) 2003 *Protecting Water Quality from Urban Runoff*. http://www.epa.gov/npdes/pubs/nps_urban-facts_final.pdf.

US EPA (Environmental Protection Agency) 2008 *Reducing Urban Heat Islands: Compendium of Strategies*. http://www.epa.gov/heatisland/resources/compendium.htm.

Van Rees, K. C. & Comerford, N. B. 1986 Vertical root distribution and strontium uptake of a slash pine stand on a Florida spodosol. *Soil Science Society of America Journal* **50**, 1042–1046.

Yeh, P. J. F. & Eltahir, E. A. B. 2005 Representation of water table dynamics in a land surface scheme. Part I: model development. *Journal of Climate* **18** (12), 1861–1880.

Zhang, L., Dawes, W. R. & Walker, G. R. 2001 Response of mean annual evapotranspiration to vegetation changes at catchment scale. *Water Resources Research* **37** (3), 701–708.

First received 31 January 2014; accepted in revised form 23 June 2014. Available online 2 July 2014